Dynamics-Aware Target Following for an Autonomous Surface Vehicle Operating under COLREGs in Civilian Traffic

Petr Švec[1], *Member, IEEE*, Brual C. Shah[1], Ivan R. Bertaska[2], Jose Alvarez[2], Armando J. Sinisterra[2],
Karl von Ellenrieder[2], *Member, IEEE*, Manhar Dhanak[2], and Satyandra K. Gupta[3], *Senior Member, IEEE*

Abstract— We present a model-predictive trajectory planning algorithm for following a target boat by an autonomous unmanned surface vehicle (USV) in an environment with static obstacle regions and civilian boats. The planner developed in this work is capable of making a balanced trade-off among the following, possibly conflicting criteria: the risk of losing the target boat, trajectory length, risk of collision with obstacles, violation of the Coast Guard Collision Regulations (COLREGs), also known as "rules of the road", and execution of avoidance maneuvers against vessels that do not follow the rules. The planner addresses these criteria by combining a search for a dynamically feasible trajectory to a suitable pose behind the target boat in 4D state space, forming a time-extended lattice, and reactive planning that tracks this trajectory using control actions that respect the USV dynamics and are compliant with COLREGs. The reactive part of the planner represents a generalization of the velocity obstacles paradigm by computing obstacles in the control space using a system-identified, dynamic model of the USV as well as worst-case and probabilistic predictive motion models of other vessels. We present simulation and experimental results using an autonomous unmanned surface vehicle platform and a human-driven vessel to demonstrate that the planner is capable of fulfilling the above mentioned criteria.

I. INTRODUCTION

Target following in a marine environment with static and dynamic obstacles such as vessels, docks, and other prohibited regions presents non-trivial trajectory planning and tracking challenges for an autonomous unmanned surface vehicle (USV) [1]. The USV may have different dynamic characteristics compared to the target boat as well as other operating vessels, and it may not know their planned course in advance. The dynamics and the current state (e.g., as defined by the pose, and the surge, sway, and yaw speeds) of the boats impose acceleration constraints that may significantly influence their braking distance and minimum turning radius. These constraints modify the set of allowable velocities, and as such may force the USV to take a different trajectory than the target boat during the follow task. In addition, the use of USVs for civil applications, especially in areas

with high traffic, entails following the Coast Guard Collision Regulations (COLREGs) [2]. These regulations, also known as the "rules of the road", define when and how to yield to other boats in the scene. They are increasingly being implemented into autonomous USV systems [3] as they are aimed to ensure greater safety in marine environments.

In order to address these challenges, a balanced trade-off needs to be made among the following criteria: the risk of losing the target boat, trajectory length, risk of collision with obstacles, violation of COLREGs, and execution of avoidance maneuvers against boats that do not follow COLREGs. The criteria can be conflicting, e.g., aggressive maneuvering shortens the trajectories but may increase the risk of collision [4] or violate COLREGs. On the other hand, overly conservative, long trajectories may cause losing the target boat and are less fuel efficient in general.

We have developed an integrated, model-predictive trajectory planning approach for the USV in the form of a follow behavior that has the capability to provide this trade-off. The planner developed in this work tightly integrates deliberative and reactive trajectory planners as well as a lower-level feedback controller to allow efficient, safe, and COLREGs-compliant target boat following.

The deliberative planner (see Section V-A) addresses the minimal trajectory length, the risk of losing the target boat, and the risk of collision with obstacles criteria. It computes a trajectory between the current pose of the USV and a suitable pose represented as a motion goal behind the target boat. The trajectory is dynamically feasible and thus directly executable by the autonomous system. It attempts to minimize the risk of collision at a higher level by searching in a 4D state space forming a time-extended lattice that captures the estimated, future motion of obstacles.

The reactive, COLREGs-compliant planner (see Section V-D) fulfils the remaining criteria. It determines the desired surge speed and heading control commands so that the USV follows the nominal trajectory. It identifies a subset of dynamically feasible control actions that may lead to collisions with obstacles by forward-simulating a system-identified, non-linear dynamic model of the USV (see Section IV). It thus represents a generalization of the velocity and acceleration based obstacle avoidance approaches [5] to systems with non-linear dynamics and advanced motion control methods. The control-imposed collision regions are expanded to enforce COLREGs-compliant guidance. The planner can be characterized as reciprocal [5], i.e., it utilizes worst-case and probabilistic predictive motion models of

[1]P. Švec and Brual C. Shah are with the Department of Mechanical Engineering, University of Maryland, College Park, MD 20742, USA {petrsvec,brual}@umd.edu

[2]I.R. Bertaska, J. Alvarez, A.J. Sinisterra, K. Ellenrieder, and M. Dhanak are with the Department of Ocean & Mechanical Engineering, Florida Atlantic University, Dania Beach, FL 33004-3023 {ibertask,jalvar36,asiniste,ellenrie,dhanak}@ fau.edu

[3]S.K. Gupta is with the Department of Mechanical Engineering and Institute for Systems Research, University of Maryland, College Park, MD 20742, USA skgupta@umd.edu

obstacles to make assumptions about their future motion. This leads to more optimal vehicle motion, i.e. by removing undesirable oscillations in the execution of its control actions and by providing a way to reason about the mutual responsibility of the boats in collision avoidance. We provide a formalism for the characterization of these models. Finally, the planner is capable of executing avoidance maneuvers to avoid collision with aggressive vessels that do not follow COLREGs.

We have carried out experiments in simulation as well as with our autonomous unmanned surface vehicle platform and a human-driven vessel (see Section VI).

II. RELATED WORK

A comprehensive survey of the state-of-the-art motion control approaches for non-adversarial following of a moving target boat is presented in [6]. This includes high-speed tracking with precise maneuverability [7], the MESSIN system [8] that combines target following with reactive obstacle avoidance, cooperative control [9] approach for multiple vehicles that is validated using DELFIMX and Aguas Vivas platforms, master boat following with two physical USVs [10], and formation control in the presence of ocean disturbances [11]. In summary, the approaches consider one or more autonomous boats following the trajectory of the target boat in an environment without obstacles and assume that the USV has the same motion characteristics as the target boat.

Current USV platforms utilize obstacle avoidance to move between waypoints, e.g., as in the guidance system developed by SPAWAR [12]. A recent survey of trajectory planning under nonholonomic constraints can be found in [13]. This includes trajectory planning using Maneuver Automaton (MA) that was adapted in [14], [15], and [16] for computation of dynamically feasible trajectories for surface vehicles. In this paper, we include time as an additional state variable to capture the motion of dynamic obstacles. On the lower, reactive level, Wilkie et al. [17] introduced a generalized velocity obstacles (GVO) algorithm for obstacle avoidance that accounts for vehicle kinematics.

A survey of trajectory planning techniques compliant with COLREGs can be found in [3]. Here, we present only the most significant contributions that closely resemble our planning approach. Benjamin's interval programming (IP) based behavior architecture was presented in [18] for weighted blending of action outputs of behaviors implementing COLREGs. In this architecture, each behavior generates a single objective function over the actuator's space of the vehicle that are combined to produce a single control action for execution. Larson et al. [19] combined the velocity obstacles (VO) algorithm with a method for computing trapezoidal projected regions which moving obstacles could occupy along their future trajectories. The shape of the projected obstacle area is skewed to comply with COLREGs. Similarly, Kuwata et al. [20] also combined VO with COLREGs and incorporated it into NASA JPL's CARACaS control architecture. The approach presents few extensions such as pre-collision check using Closest Point of Approach (CPA), handling uncertain

obstacle motion by applying a safety buffer, and incorporating hysteresis into control action execution.

In contrast to the previous approaches, our planning algorithm uses a system-identified, non-linear USV dynamic model for COLREGs-compliant target following. The algorithm is capable of predicting the future motion choices of obstacles using worst-case and probabilistic predictive motion models (i.e., we do not make simplifying assumptions about the motion of obstacles). This is mostly useful when operating in congested waters containing boats with different dynamics and possibly conflicting intentions. Finally, the algorithm combines the deliberative and reactive trajectory planning to prevent getting trapped in a local minima.

III. PROBLEM FORMULATION

The task for the model-predictive planner is to determine the minimum cost, collision-free control commands (i.e., desired surge speed u and heading ψ) for the USV to approach the target boat. More formally, given,

(i.) the continuous state space $\mathcal{X} = \mathcal{X}_\eta \times \mathcal{X}_\nu \times \mathcal{T}$ in which each state $\mathbf{x} = [\eta^T, \nu^T, t]^T$ consists of the vehicle's pose $\eta = [x, y, \psi]^T \in \mathcal{X}_\eta \subseteq \mathbb{R}^2 \times \mathbb{S}^1$, velocity $\nu = [u, v, r]^T \in \mathcal{X}_\nu \subseteq \mathbb{R}^3$, and the time t. The pose η consists of x and y position coordinates, and the orientation ψ of the vehicle about the z-axis in the North-East-Down (NED) coordinate system [21]. The velocity vector ν consists of the surge u, sway v, and angular r speed about the z axis in NED (i.e., we neglect the heave, roll, and pitch motion components);

(ii.) the current state of the USV $\mathbf{x_U} = [\eta_\mathbf{U}{}^T, \nu_\mathbf{U}{}^T, t]^T \in \mathcal{X}$ and the moving target $\mathbf{x_T} = [\eta_\mathbf{T}{}^T, \nu_\mathbf{T}{}^T, t]^T \in \mathcal{X}$;

(iii.) the continuous, state-dependent, control action space $\mathcal{U}_c(\mathbf{x}) \subset \mathbb{R}^2 \times \mathbb{S}^1$ of the USV in which each control action $\mathbf{u_c} = [u_d, \psi_d]^T$ consists of the desired surge speed u_d and heading ψ_d in NED;

(iv.) 3 degrees of freedom dynamic model of the USV $\dot{\mathbf{x}}_\mathbf{U} = f_U(\mathbf{x_U}, \mathbf{u_h})$, where the thrust and moment are produced by model actuators that take $\mathbf{u_h}$ as the control input. This control input is determined by the controller $h_U(\mathbf{x_U}, \mathbf{u_c}, P_U)$, where P_U is the set of controller parameters;

(v.) The geometric region $\mathcal{O}_s = \bigcup_{k=1}^K o_{s,k} \subseteq \mathbb{R}^2$ occupied by static obstacle;

(vi.) The dynamic obstacles and their estimated states $\{\mathbf{x_{o,l}} | \mathbf{x_{o,l}} \in \mathcal{X}\}_{l=1}^L$, the geometric region occupied by the obstacles $\mathcal{O}_d = \bigcup_{l=1}^L o(\mathbf{x_{o,l}}) \subseteq \mathbb{R}^2$, and their worst-case $\mathcal{M}_w = \bigcup_{l_1=1}^{L_1} m_{w,l_1}$ and probabilistic $\mathcal{M}_p = \bigcup_{l_2=1}^{L_2} m_{p,l_2}$ predictive motion models, where $L_1 + L_2 \leq L$. The models take the state $\mathbf{x_{o,l}}(t)$ of the obstacle l at the time t as the input and produces a set of possible states $\mathcal{X}_{o,t+\Delta t}$ occupied by the obstacle at the time $t + \Delta t$; and

(vii.) the required operating distance l_G of the USV from the target boat.

Compute,

(i.) a motion goal $\eta_\mathbf{G} = [x_G, y_G, \psi_G]^T \in \mathcal{X}_\eta$ positioned l_G distance from the target boat;
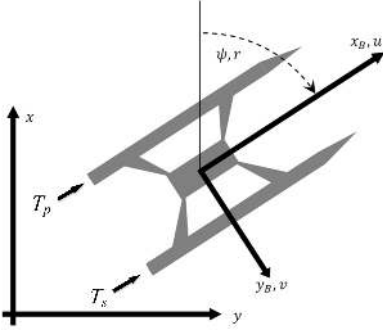
Fig. 1: USV14 body-fixed coordinate system.

Fig. 2: Waypoint following simulation of the USV14 at a nominal surge speed of 2 m/s.

(ii.) a collision-free, dynamically feasible trajectory τ : $[0, T] \to \mathcal{X}_{\eta, free}$ such that $\tau(0) = \eta_{\mathbf{U}}$, $\tau(T) = \eta_{\mathbf{G}}$ and the execution time T is minimized. Each state $\eta_{\mathbf{U}}(t) = [x_t, y_t, \psi_t]^T$ along τ thus represents a geometric transformation of the USV in the free state space $\mathcal{X}_{\eta, free} = \mathcal{X}_\eta \backslash \mathcal{X}_{\eta, obs} = \{\eta_{\mathbf{U}}(t) \in \mathcal{X}_\eta | U(\eta_{\mathbf{U}}(t)) \cap \mathcal{O}(t) = \emptyset\}$ (also known as a free configuration space $C_{free} = \mathcal{X}_{\eta, free}$) for $t \in [0, T]$, where $\mathcal{O}(t) = \mathcal{O}_s(t) \cup \mathcal{O}_d(t)$ and $U(\eta_{\mathbf{U}}(t)) \subseteq \mathbb{R}^2$ is a geometric region occupied by the USV U in $\eta_{\mathbf{U}}(t)$;

(iii.) a desired, COLREGs-compliant control action $\mathbf{u}_{\mathbf{c}}^*$ for the USV to track τ to advance towards $\eta_{\mathbf{G}}$, while avoiding dynamic obstacles.

The USV experiences uncertain ocean wave- and wind-induced motion disturbances, which may cause it to drift towards obstacles. Hence, the motion goal $\eta_{\mathbf{G}}$, trajectory τ, as well as the desired control action $\mathbf{u_c}$ need to be recomputed with a high frequency to keep track of the moving target, and to handle dynamic obstacles and pose errors. A Kalman filter is used to determine the vehicle state from multiple sensors [22].

IV. DYNAMIC USV MODEL

The vessel utilized for testing of the planner is named the WAM-V USV14. The physical characteristics of this vehicle are given in Section VI-B. A three degree of freedom (surge x_B, sway y_B and yaw ψ, see Fig. 1) dynamic simulation of the USV14 was created. The origin of the body-fixed coordinate system is fixed at the USV's center of gravity. With these assumptions, the equations of motion in the body-fixed frame can be reduced as in [21]:

$$
\begin{aligned}
X &= (m - X_{\dot{u}})\dot{u} - (m - Y_{\dot{v}})vr + Y_{\dot{r}}r^2 - X_u u, \\
Y &= (m - Y_{\dot{v}})\dot{v} - Y_{\dot{r}}\dot{r} + (m - X_{\dot{u}})ur - Y_v v - Y_r r, \\
N &= (I_z - N_{\dot{r}})\dot{r} - Y_{\dot{r}}\dot{v} + (X_{\dot{u}} - Y_{\dot{v}})uv - Y_{\dot{r}}ur \\
&\quad - N_v v - N_r r,
\end{aligned}
\tag{1}
$$

where (u,v,r) are the vehicle's surge speed, sway speed, and yaw rate, respectively, m is the vehicle's mass, and I_z is the mass moment of inertia about the z-axis. X and Y are the control forces in the x_B and y_B directions, respectively, and N is the control moment about the z_B axis. The uppercase values are drag and added mass coefficients
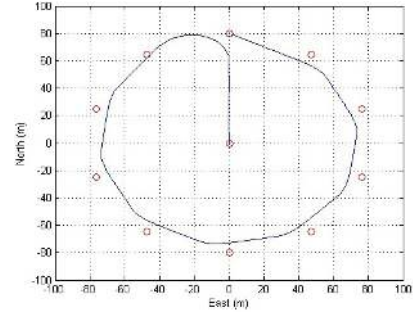
that relate subscripted terms to the uppercase terms, e.g., X_u is the drag coefficient in the x_B direction due to the surge velocity and $X_{\dot{u}}$ is the hydrodynamic coefficient relating the acceleration in the x_B direction to the force in the x_B direction [21].

The USV14 is an under-actuated vehicle with control forces and moments acting only in the surge and yaw degrees of freedom. The USV relies on differential thrust for steering. A benefit of this is that forward speed is not required to execute turning maneuvers. However, heading control cannot be decoupled from the surge speed, and the maximum moment generated by the propellers is inversely dependent on the thrust. Taking these factors into account, the equations of motion in (1) can be expanded to include the applied forces and moments,

$$
\begin{aligned}
X &= T_p + T_s, \\
Y &= 0, \\
N &= (T_p - T_s)\frac{l}{2},
\end{aligned}
\tag{2}
$$

where T_p and T_s denote the thrust from the port and starboard waterjets, respectively, and l is the separation distance between the centerline of each hull. Using (1) and (2), a dynamic simulation of the vehicle was created. Building upon this model, a heading and speed controller analogous to the one implemented on the vehicle was created with a PD controller. This was expanded to include a line-of-sight (LOS) guidance system. An example of the vehicle following a trajectory can be found in Fig. 2.

V. FOLLOW BEHAVIOR

The developed algorithm for following a target boat consists of deliberative trajectory planning, and reactive, COLREGs-compliant obstacle avoidance components in our guidance, navigation, and control (GNC) system architecture.

A. Deliberative Trajectory Planning

The trajectory planner searches for a collision-free, dynamically feasible trajectory $\tau : [0, t] \to \mathcal{X}_{\eta, free} \times \mathcal{T}$ between $\eta_{\mathbf{U}}$ and $\eta_{\mathbf{G}}$ poses of the USV. The motion goal $\eta_{\mathbf{G}} = [x_T - l_G cos\psi, y_T - l_G sin\psi, \psi_T]^T$ is a projection of the target's position $[x_T, y_T]^T$ to a location behind the USV at the distance l_G.
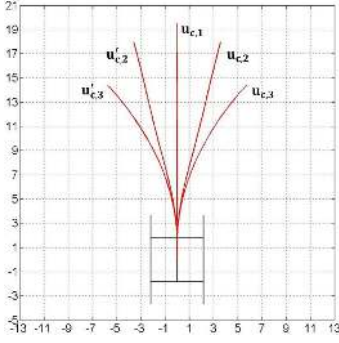
Fig. 3: An example of the control action set $\mathcal{U}_{c,d}$ for the USV14 nominal surge speed of 2 m/s.

Fig. 4: Heading controller of the USV14 (WAM-V).

We discretize $\mathcal{X}_\eta \times \mathcal{T}$ into the state space $\mathcal{S}$ for trajectory planning. Each discrete state $\mathbf{s_j} = [x_j, y_j, \psi_j, t_j]^T$ thus represents a 4D cube in $\mathcal{S}$. We also define a discrete space $\mathcal{U}_{c,d}(\mathbf{s_j}) \subseteq \mathcal{U}_c(\mathbf{x_j})$ of dynamically feasible control action primitives (see Fig. 3). A discrete control action primitive $\mathbf{u_{c,d,k}} \in \mathcal{U}_{c,d}$ is represented as a sequence $\{\eta_{\mathbf{i}}\}_{i=1}^{L_k}$ of USV poses in $\mathcal{X}_\eta \times \mathcal{T}$ and is determined using the dynamic model of the USV (see Section IV). The model is used to determine neighboring states that can be reached by the vehicle for a given time and constant speed.

The search is carried out over a 4D lattice structure L : $\mathbf{s_j}, \mathbf{u_{c,d,k}} \rightarrow \mathbf{s_{j,k}}$ that maps states $\mathbf{s_j} \in \mathcal{S}$ to their neighboring states $\mathbf{s_{j,k}}$ using discrete control action primitives $\mathbf{u_{c,d,k}} \in \mathcal{U}_{c,d}(\mathbf{s_j})$ for $j = 1, 2, \ldots, |\mathcal{S}|$, and $k = 1, 2, \ldots, |\mathcal{U}_{c,d}(\mathbf{s_j})|$. Each layer in L thus represents a specific 2D planning space with the fixed heading ψ of the USV and time t. The final state $\mathbf{s_{j,k}}$ of the primitive (in the body frame of the USV) is conveniently selected to be in the center of its corresponding cube (i.e., to preserve the continuity of τ). The lattice representation reduces the computational demand of the search, while explicitly considering the differential constraints of the vehicle. It is up to the user of the planner to determine the resolution of the state space, the number of control action primitives, and their shape.

The lattice is constructed incrementally while searching for the trajectory. The states are expanded in the least-cost, heuristic, weighted A* fashion [13] according to the cost function $f(\mathbf{s}) = g(\mathbf{s}) + \epsilon h(\mathbf{s})$ in which $g(\mathbf{s})$ is the optimal *cost-to-come* from $\mathbf{s_U}$ (a discrete pose of the USV) to $\mathbf{s}$, $h(\mathbf{s})$ is the heuristic *cost-to-go* between $\mathbf{s}$ and $\mathbf{s_G}$ (a discrete motion goal), and ϵ is the inflation factor. The *cost-to-come* is computed as $g(\mathbf{s}) = \sum_{k=1}^{K} l(\mathbf{u_{c,d,k}})$ over K planning stages, where $l(\mathbf{u_{c,d,k}})$ is the actual execution time of $\mathbf{u_{c,d,k}}$ (we assume that the USV will execute the trajectory with its maximum allowable speed). It is set to ∞ if the primitive makes the USV transition to the obstacle region $\mathcal{S}_{obs} \subseteq \mathcal{S}$. The heuristic $h(\mathbf{s})$ is expressed as the required time to reach $\mathbf{s_G}$ along a straight line from $\mathbf{s}$. The heuristic increases the speed of the search by focusing on the most promising regions of the state space, while still allowing resolution-optimal planning. The inflation factor $\epsilon \geq 1$ permits delicate balance between the computational
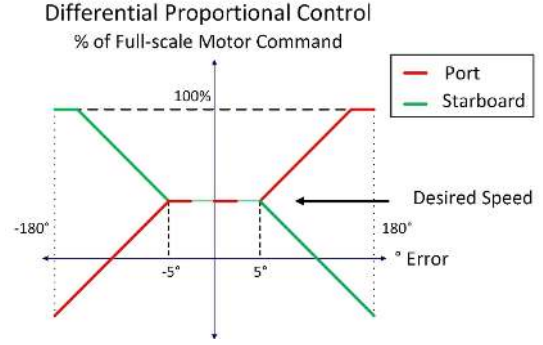
demand of the planner and the optimality of the trajectory to be achieved. The computed trajectory τ is translated into a sequence of waypoints $\{\mathbf{w_i} | \mathbf{w_i} = [x, y]^T\}_{i=1}^{N}$ serving as local motion goals for the reactive planner.

B. Waypoint Following

The vehicle utilizes a LOS guidance system driven by a proportional heading controller for trajectory following. Due to the differential steering, the vehicle heading controller differs from those that utilize rudder steering systems as in [21]. Differential steering imposes a moment about the vehicle that causes it to turn. With this configuration, the controller manages vehicle direction by two separate proportional control laws. Each of these controllers focuses on a single motor, with the only difference being that the slope of one line is the opposite of the other. To better handle real world scenarios, a tolerance region is implemented where the error is less than five degrees. This is to account for natural vehicle variation in response to wind and wave forces. Fig. 4 displays the proportional control law, wherein the port and starboard thrust of the vehicle are controlled by separate commands that denote a percentage of the full-scale value of thrust. An offset is introduced into the motor command output of the controller, corresponding to the desired speed of the vehicle. This offset can fluctuate in response to the speed error multiplied by a gain, constituting the speed p-controller. The structure and implementation of the vehicle controller is similar to that found in [23].

C. Predictive Motion Models of Dynamic Obstacles

The behavior of a dynamic obstacle is characterized by a policy $\pi(\mathbf{x_o}) : \mathcal{X} \rightarrow \Theta_c$ that determines a desired control action $\theta_{\mathbf{c}} \in \Theta_c(\mathbf{x_o})$ for each obstacle's state $\mathbf{x_o} \in \mathcal{X}$, and is generally unknown to the USV. Hence, it is either estimated from the sequence of the past observed obstacle's states $\{\mathbf{x_o}(t), \mathbf{x_o}(t-1), \ldots, \mathbf{x_o}(t-\Delta t)\}$, or through a priori knowledge of the desired goal states (e.g., through direct communication with the vessel). In both the cases, the set of possible future states of the obstacle can be computed using either worst-case or expected-case analysis, resulting in corresponding models.

The worst-case model m_w predicts possible future obstacle states $\mathcal{X}_{o,t+\Delta t}(\mathbf{x_o}(t)) = \{\mathbf{x_o}(t + \Delta t) \in$

$\mathcal{X} | \exists \theta_{\mathbf{c}}(t) \in \Theta_c(\mathbf{x_o}(t))$ such that $\mathbf{x_o}(t + \Delta t) = \mathbf{x_o}(t) + \int_t^{t+\Delta t} f_o(\mathbf{x_o}(t'), \theta_{\mathbf{h}}(t'))dt'$, and $\theta_{\mathbf{h}}(t) = h_o(\mathbf{x_o}(t), \theta_{\mathbf{c}}(t), P_o)\}$ (e.g., simplified as a triangular region for the vessel 1 in Fig. 5a)) that can be reached by the obstacle at the time $t + \Delta t$. We simplify the notation by assuming that the obstacle will start executing the control action $\theta_{\mathbf{c}}(t)$ at the time t and will keep it constant for the entire time interval (i.e., the obstacle does not switch between different control actions within this interval). By using this model, the USV does not have any preferences about the obstacle's future motion. It can only estimate a set of its reachable future states given the inferred obstacle's dynamic model $\dot{\mathbf{x}}_{\mathbf{o}} = f_o(\mathbf{x_o}, \theta_{\mathbf{h}})$ and corresponding controller $h_o(\mathbf{x_o}, \theta_{\mathbf{c}}, P_o)$.

The probabilistic model generalizes the worst-case model by defining a probability distribution $P(\mathbf{x_o}(t + \Delta t) | \mathbf{x_o}(t)) = \sum_{\theta_{\mathbf{c}}(t) \in \Theta_c(\mathbf{x_o}(t))} P(\theta_{\mathbf{c}}(t) | \mathbf{x_o}(t + \Delta t) = \mathbf{x_o}(t) + \int_t^{t+\Delta t} f_o(\mathbf{x_o}(t'), \theta_{\mathbf{h}}(t'))dt'$, and $\theta_{\mathbf{h}}(t') = h_o(\mathbf{x_o}(t'), \theta_{\mathbf{c}}(t'), P_o))$ over the obstacle's possible future states. This model is very general and can be used to represent the obstacle's intentions to satisfy COLREGs in different states. By using this model, the USV has more flexibility, i.e., it can balance between the time required to reach its goal and the probability of collision.

D. COLREGs-Compliant Obstacle Avoidance

Here, we present a reactive, COLREGs-compliant planning algorithm for avoiding dynamic obstacles. The algorithm determines a control action that respects the USV dynamics, minimizes the probability of a collision, and optimizes the time needed to reach a local waypoint. The planner utilizes predictive motion models of obstacles (see Section V-C) when evaluating candidate control actions.

In each planning step, the planner first determines a set of control actions $\mathcal{U}_{c,free}(\mathbf{x_U}) = \mathcal{U}_c(\mathbf{x_U}) \backslash \mathcal{U}_{c,obst}(\mathbf{x_U})$ that allow the USV to avoid collision zones. The set $\mathcal{U}_{c,obst}$ thus defines obstacles in the control space and is determined by sampling $\mathcal{U}_c$, forward simulating the control actions using $\dot{\mathbf{x}}_{\mathbf{U}} = f_U(\mathbf{x_U}, \mathbf{u_h})$ up to the time horizon t_{max}, where $\mathbf{u_h} = h_U(\mathbf{x_U}, \mathbf{u_c}, P_U)$, and checking for possible collisions. $\mathcal{U}_{c,obst}$ thus generalizes the velocity obstacles paradigm [17]. More precisely, the set $\mathcal{U}_{c,obst}(\mathbf{x_U}) = \{\mathbf{u_c} | d_{CPA}(t_{max}) < d_{CPA,col}\}$, where $d_{CPA}(t_{max})$ is the minimum distance between the closest point of approach (CPA) (i.e., the location from which the USV has the minimum distance from obstacles) and obstacles when $\mathbf{u_c}$ is executed from $\mathbf{x_U}$ for the time horizon t_{max}. The distance $d_{CPA}(t_{max})$ is defined as $d_{CPA}(t_{max}) = \min_{t \in [0, t_{max}]} \| U(\eta_{\mathbf{U}}(t)) - \mathcal{O}(t)) \|$, where $U(\eta_{\mathbf{U}}(t))$ is the geometric region in $\mathbb{R}^2$ occupied by the USV at $\eta_{\mathbf{U}}(t)$, and $\mathcal{O}(t)$ is a region of time-projected obstacles. The parameter $d_{CPA,col}$ defines the distance threshold from an obstacle, and it can be adjusted to serve as a safety factor to handle motion and sensing uncertainties.

It is important to note that the computation of d_{CPA} is performed with respect to the region occupied by the obstacles at their possible future states, as defined by their worst-case or probabilistic models. Hence, in case of the worst-case model,

the region occupied by a single obstacle at the time $t + \Delta t$ is $o(t + \Delta t) = \bigcup_{\mathbf{x_o}(t+\Delta t) \in \mathcal{X}_{o,t+\Delta t}} o(\mathbf{x_o}(t + \Delta t))$, where $o(\mathbf{x_o}(t + \Delta t))$ is the region occupied by the obstacle at the state $\mathbf{x_o}(t+\Delta t)$. The notation is similar for the probabilistic model with the exception that $o(\mathbf{x_o}(t + \Delta t))$ is the region occupied by the obstacle at the state $\mathbf{x_o}(t+\Delta t) \in \mathcal{R}_{o,t+\Delta t} \subseteq \mathcal{X}_{o,t+\Delta t}$. The subset $\mathcal{R}_{o,t+\Delta t}$ specifies the states that will be reached by the obstacle with the probability $p \geq p_{min}$, where p_{min} is the user-specified threshold.

As the next step of the algorithm, the planner determines whether the USV, given its current pose, is in a COLREGs situation with respect to all other vessels. This is determined using $d_{CPA}(t_{max}) < d_{CPA,min}$ and $t_{CPA}(t_{max}) < t_{CPA,max}$ condition, where $d_{CPA,min}$ and $t_{CPA,max}$ are the user-specified distance and time thresholds. The time to CPA $t_{CPA}(t_{max})$ is defined as $t_{CPA}(t_{max}) = \text{argmin}_{t \in [0, t_{max}]} \| U(\eta_{\mathbf{U}}(t)) - \mathcal{O}(t) \|$. The variable $d_{CPA}(t_{max})$ is computed for the control action $\mathbf{u_c} = [u_d, 0]^T$ up to the maximum look-ahead time t_{max}, where u_d is the current surge speed of the USV.

If the above defined condition holds, the USV determines which one of the following COLREGs situations, i.e., "head-on", "crossing", and "overtaking" [2] is valid with respect to all obstacles. This is useful for determining what constraints to apply on $\mathcal{U}_{c,free}$ to make the USV act according to the user's needs in a particular COLREGs situation. Fig. 8 illustrates the COLREGs situations. Let $b_{U,o} = 2\pi + \arctan(y_U - y_o/x_U - x_o) - \arctan(n_{o,y}/n_{o,x})$ be the relative bearing of the USV to the dynamic obstacle, where $\hat{\mathbf{n}}_o = [n_{o,x}, n_{o,y}]^T$ is the unit vector in the direction of the obstacle's heading ψ_o. Let $h_{U,o} = 2\pi + \arctan(n_{U,y}/n_{U,x}) - \arctan(n_{o,y}/n_{o,x})$ be the relative heading of the USV to the obstacle, where $\hat{\mathbf{n}}_U$ is the unit vector in the direction of the USV's heading ψ_U. Both the values are required to be within $[0, 2\pi)$. The "head-on" situation is activated if $b_{U,o} \in [b_{h,min}, b_{h,max}]$, $h_{U,o} \in [h_{h,min}, h_{h,max}]$, the relative, along-track x coordinate of the obstacle in the body-fixed coordinate system of the USV satisfies $x_{o,U} \geq x_{h,min}$, and the relative, cross-track y coordinate of the obstacle satisfies $|y_{o,U}| \leq y_{h,max}$. The "crossing" situation is activated if $b_{U,o} \in [b_{c,min}, b_{c,max}]$, $h_{U,o} \in [h_{c,min}, h_{c,max}]$, and $x_{o,U} \geq x_{c,min}$. The "overtaking" situation is activated if $h_{U,o} \in [h_{o,min}, h_{o,max}]$, $x_{o,U} \geq x_{o,min}$, and $|y_o| \leq y_{o,max}$.

If the USV is in a COLREGs situation with respect to any of the obstacles, the collision-free control actions $\mathcal{U}_{c,free}$ are divided into COLREGs-compliant control actions $\mathcal{U}_{c,COLREGs}$ and control actions $\mathcal{U}_{c,\neg COLREGs}$ that do not respect COLREGs. The subset $\mathcal{U}_{c,COLREGs}$ is determined based on the type of the current COLREGs situation and the future-projected possible states of obstacles relative to the current state of the USV. Let $\eta_{\mathbf{o}}(t)$ be the pose of the obstacle at the projected time t. Let $\eta_{\mathbf{U}}(t_0)$ and $\eta_{\mathbf{U}}(t)$ be the poses of the USV at the current and the projected time (after executing a control action $\mathbf{u_c}$), respectively. Let $\hat{\mathbf{n}}_{U,t_0,t}$ be the unit vector in the direction between $\eta_{\mathbf{U}}(t_0)$ and $\eta_{\mathbf{U}}(t)$. Let $\hat{\mathbf{n}}_{U,o} = [n_{U,o,x}, n_{U,o,y}]^T$ be the unit vector in the direction between $\eta_{\mathbf{U}}(t_0)$ and $\eta_{\mathbf{o}}(t)$. Then, the con-

trol action $\mathbf{u_c}$ is considered to be COLREGs-compliant if $([n_{U,o,y}, -n_{U,o,x}]^T \cdot \hat{\mathbf{n}}_{U,t_0,t}) < 0$, i.e., it leads the USV to the right half-plane between its current pose and the future projected pose of the obstacle.

The desired control action $\mathbf{u_c^*} = \arg\min_{\mathbf{u_c}=[u_d,\psi_d]^T \in \mathcal{U}_{c,free}(\mathbf{x_U})} \omega_u((u_{d,max} - u_d)/u_{d,max}) + (1-\omega_u)(|\psi_{\mathbf{w_j}} - \psi_d|/2\pi) + p_{COLREGs}$ is then selected that directs the USV towards one of the trajectory waypoints $\mathbf{w_j}$. Here, $u_{d,max}$ is the maximum surge speed of the USV, $\psi_{\mathbf{w_j}}$ is the heading towards $\mathbf{w_j}$, and ω_u is the user-specified weight of the surge speed error with respect to the heading error. The variable $p_{COLREGs} = \frac{\omega_{CPA,t}}{t_{CPA}} + \frac{\omega_{CPA,d}}{d_{CPA}}$ represents additional penalty for a control action that is not COLREGs-compliant (otherwise it is equal to zero), where $\omega_{CPA,t}$ and $\omega_{CPA,d}$ are user-specified weights.

In general, the control actions are selected and evaluated with respect to all surrounding obstacles. The control actions that lead to COLREGs-compliant guidance are strictly preferred. However, the USV can still breach the rules if no COLREGs-compliant action is available.

VI. SIMULATION AND EXPERIMENTAL RESULTS

A. Simulation Results

We present a simulation result of the USV14 operating in an environment with three civilian boats (see Fig. 5). The waypoint for the USV ($\mathbf{w_U}$) is at the top of the experimental scene and marked with a black empty circle. The waypoint ($\mathbf{w_1}, \mathbf{w_2}$, and $\mathbf{w_3}$) for each obstacle vessel is marked as a red circle with a cross inside it. The maximum surge speed of the USV is 5 m/s. The speed of the vessel 1 is 4 m/s and the speed of the vessels 2 and 3 is 1 m/s. During the operation, the USV had to deal with the "head-on" and "crossing from right" situations first by yielding to the vessels 1 and 2, respectively, as shown in Fig. 5a) and b). After yielding to the vessel 2, the USV was in an "overtaking" situation with respect to the vessel 3 (see Fig. 5c)). It correctly avoided crossing vessel 3 on its starboard as prescribed by COLREGs and finally reached its goal (see Fig. 5d)).

In this experiment, the USV forward simulates its control actions for the look-ahead time $t_{max} = 20$ s. This results in a set of projected USV positions, where the positions that correspond to the subset of control actions leading to a collision region are marked using red crosses (see Fig. 5a). The projected positions breaching COLREGs are marked as blue plus signs. The green circles result from the execution of control actions that do not lead the USV to the collision region. Each control action has assigned a cost as described in Section V-D and the USV selects the one with the minimum value. The values of parameters for the planner were selected as follows $d_{CPA,col} = 20$ m, $d_{CPA,min} = 100$ m, $t_{CPA,max} = 30$ s, $u_{d,max} = 5$ m/s, $\omega_u = 0.55$, $\omega_{CPA,t} = 50$, and $\omega_{CPA,d} = 100$.

The control action set consisted of 140 control actions with 10 levels of the desired surge speed between 0 and 5 m/s and 14 levels of heading angles starting from -105 to 105 degrees in the body frame of the USV. The computational demand of our C++ implementation for computing and evaluating this
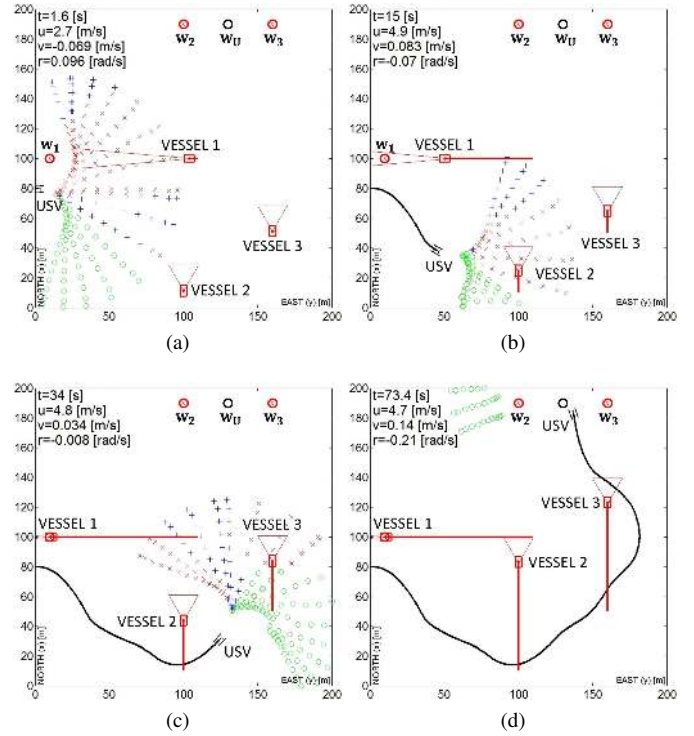

Fig. 5: The result of a simulation experiment during which the USV was required to resolve a "head-on" situation with respect to the vessel 1 (see a)), "crossing from right" situation with respect to the vessel 2 (see a) and b)), and "overtaking" situation with respect to the vessel 3 (see c) and d)).

set was below 0.6 s on Intel(R) Core(TM) i7-2600 CPU @ 3.4 GHz machine with 8 GB RAM. The computational expense scales linearly in the number of considered obstacles.

In this experiment, we only consider worst-case predictive motion models for the obstacles. In this case, the USV expects the vessel 1 to preserve its course with a small maximum deviation of its heading angle of 5 degrees (the region of the vessel's time-projected positions is simplified as a thin, red triangle in Fig. 5a). However, the USV has lower confidence in the heading of the other two vessels. It considers the maximum deviation in their heading angle to be 30 degrees.

B. Experimental Results

We present an experimental result[1] of the USV14 autonomously following a manually driven target boat in an environment with static obstacles. We also present results of the USV14 avoiding a civilian vessel in accordance with COLREGs in "head-on", "crossing from right", as well as, "overtaking" situations. The experiments were carried out with an assumption that the USV14 knows the GPS coordinates of both the target boat and the civilian vessel.

The USV14 is a 14 foot (4.3 m) long catamaran unmanned surface vehicle as shown in Fig. 6a). The vehicle is propelled

[1]The video demonstrating the simulation as well as experimental results can be found at http://youtu.be/LTwZwjT8o58

(a)   (b)

Fig. 6: (a) The autonomous USV14; (b) The human-controlled johnboat.

using two electrically-driven waterjets that are capable of producing a combined total thrust of 205 N. The platform was operated at a maximum speed of 1.7 m/s during the experiments. The johnboat (see Fig. 6b) was used as the target boat in the follow task experiment and the civilian boat in the COLREGs-compliant obstacle avoidance experiments. The boat is equipped with a 3.7 kW outboard motor that provides the top speed of 3.5 m/s.

The state estimation for the USV14 and johnboat was performed using MTi-G and MTi-G-700 sensing units, respectively. The units incorporate a wide area augmentation system (WAAS) that enables global positioning using GPS. The GPS coordinates are internally filtered to give an accurate pose and speed of the vehicle. The USV14 receives the state information from the target or traffic vessel using RF communication channels. We used the Lightweight Communications and Marshalling (LCM) message passing architecture [24] to facilitate data sharing between the different components of the autonomous system.

The experimental result of the follow task is shown in Fig. 7. In the experiment, the USV14 employed the deliberative trajectory planner to compute a dynamically feasible trajectory to a motion goal positioned 30 m directly behind the target boat. The trajectory respected the target's heading. The vehicle was directed to maintain a minimum safety distance of 30 m (shown as the red ring in Fig. 7) from the target boat. As shown in Fig. 7a), the USV14 avoids a static obstacle when approaching the target from its initial location. Fig. 7b) illustrates a situation in which the target boat increases its speed, making the USV14 accelerate to its maximum speed in order to maintain the required distance. In Fig. 7c-e), the target boat quickly reduces its speed to a complete stop, which forces the USV14 to respond appropriately by quickly slowing down.

The results of the COLREGs-compliant obstacle avoidance are shown in Fig. 8. In these experiments, the USV14 employed the reactive planner to determine a dynamically feasible, COLREGs-compliant control action to approach a local waypoint of the trajectory. Figs. 8a-b) depict the result of COLREGs-compliant obstacle avoidance in the "head-on" situation. Here, the USV14 (marked as green) headed towards a virtual target vessel (marked as red) positioned in the top left corner of the scene. The civilian boat headed towards south-east. The boats were intentionally positioned to be on a collision course. The USV14 successfully yielded to

(a)   (b)

(c)   (d)
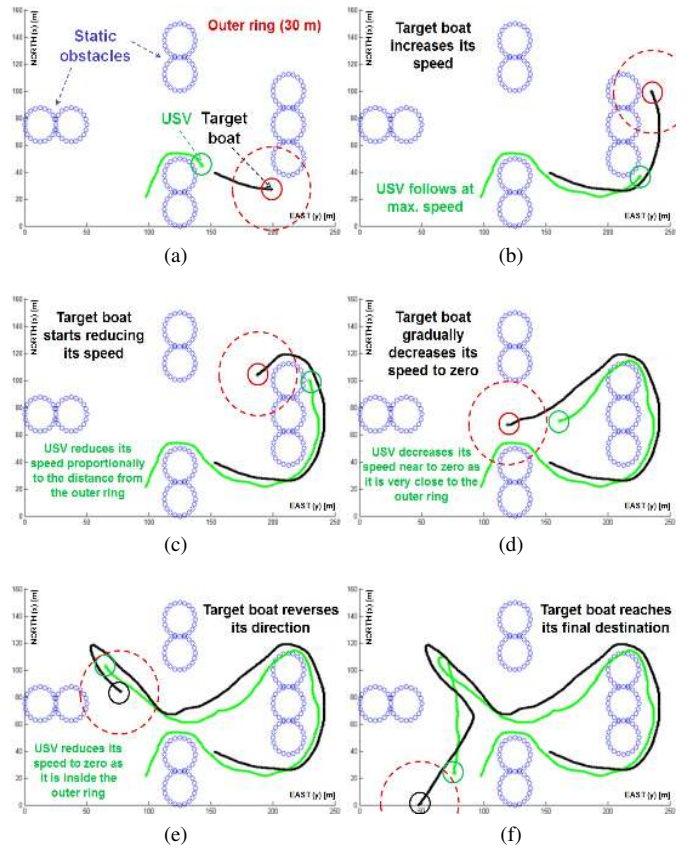
(e)   (f)

Fig. 7: The experimental result of the USV14 autonomously following the target johnboat. We use virtual obstacles with circular boundaries (shown as blue) marked by buoys to simplify the experimental setup.

the civilian boat by slowing down and steering to the right to avoid crossing from the port side of civilian vessel. Figs. 8c-d) depict the result of COLREGs-compliant avoidance in the "crossing from right" situation. In this experiment, the civilian vessel headed towards east and its speed and initial pose was set such that it was on a collision course with the USV14. Again, the USV14 successfully yielded to the civilian vessel and avoided crossing from the port side of the civilian vessel. Finally, Figs. 8e-f) depict the result of COLREGs-compliant avoidance in an "overtaking" situation. In this experiment, both the boats headed north and the speed of the civilian vessel was decreased to be between 0.5-1 m/s. The USV14 successfully carried out the required maneuver. After execution of each avoidance maneuver, the USV14 switched back to the deliberative trajectory planner and proceeded towards the virtual target vessel.

VII. CONCLUSIONS AND FUTURE WORK

In this paper, we have presented a model-predictive trajectory planning algorithm to realize dynamically feasible, COLREGs-compliant target following among civilian vessels and static obstacle regions. The combination of a discrete search in 4D state lattice and reactive planning proved capable of fulfilling the outlined task following criteria based
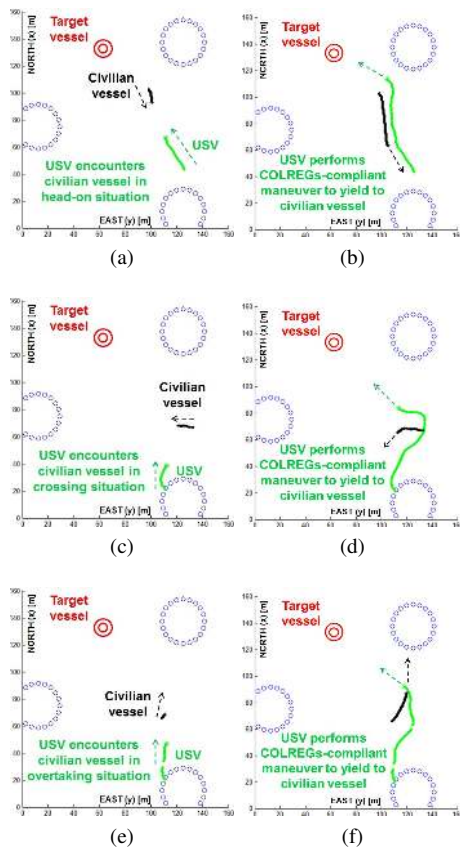
Fig. 8: The experimental results of the USV14 autonomously dealing with "head-on" (see a and b), "crossing from right" (see c and d), and "overtaking" (see e and f) situations.

on the performed simulation and physical experiments.

Our future aims are: to develop an algorithm for estimating the worst-case as well as probabilistic predictive motion models of obstacles by analyzing their past trajectories and reasoning about their possible motion goals; to incorporate machine learning for learning human-like, COLREGs-compliant obstacle avoidance strategies; to improve the computational efficiency of the planner by intelligently sampling the control action space and adaptively adjusting the simulation fidelity; to consider wind and waves disturbances directly in the planning process; and to evaluate the performance of the planner in more complex scenarios.

ACKNOWLEDGMENT

REFERENCES

[1] S. Corfield and J. Young, "Unmanned surface vehicles–game changing technology for naval operations," *Advances in unmanned marine vehicles*, pp. 311–328, 2006.

[2] U. Commandant, "International regulations for prevention of collisions at sea, 1972 ('72 COLREGs)," *US Department of Transportation, US Coast Guard, COMMANDANT INSTRUCTION M*, vol. 16672, 1999.

[3] S. Campbell, W. Naeem, and G. Irwin, "A review on improving the autonomy of unmanned surface vehicles through intelligent collision avoidance manoeuvres," *Annual Reviews in Control*, 2012.

[4] P. Švec and S. K. Gupta, "Automated synthesis of action selection policies for unmanned vehicles operating in adverse environments," *Autonomous Robots*, vol. 32, no. 2, pp. 149–164, 2012.

[5] J. van den Berg, J. Snape, S. J. Guy, and D. Manocha, "Reciprocal collision avoidance with acceleration-velocity obstacles," in *IEEE International Conference on Robotics and Automation (ICRA'11)*, 2011, pp. 3475–3482.

[6] M. Bibuli, M. Caccia, L. Lapierre, and G. Bruzzone, "Guidance of unmanned surface vehicles: Experiments in vehicle following," *IEEE Robotics & Automation Magazine*, no. 99, 2012.

[7] M. Breivik, V. Hovstein, and T. Fossen, "Straight-line target tracking for unmanned surface vehicles," *Modeling, Identification and Control*, vol. 29, no. 4, pp. 131–149, 2008.

[8] J. Majohr and T. Buch, "Modelling, simulation and control of an autonomous surface marine vehicle for surveying applications measuring dolphin messin," *IEE Control Engineering Series*, vol. 69, p. 329, 2006.

[9] A. Aguiar, J. Almeida, M. Bayat, B. Cardeira, R. Cunha, A. Häusler, P. Maurya, A. Oliveira, A. Pascoal, A. Pereira, *et al.*, "Cooperative control of multiple marine vehicles," in *Proc. of 8th IFAC International Conference on Manoeuvering and Control of Marine Craft*, pp. 16–18.

[10] M. Breivik, "Topics in guided motion control of marine vehicles," Ph.D. dissertation, Norwegian University of Science and Technology, 2010.

[11] Z. Peng, D. Wang, Z. Chen, X. Hu, and W. Lan, "Adaptive dynamic surface control for formations of autonomous surface vehicles with uncertain dynamics," *IEEE Transactions on Control Systems Technology*, no. 99, pp. 1–8, 2012.

[12] J. Larson, M. Bruch, R. Halterman, J. Rogers, and R. Webster, "Advances in autonomous obstacle avoidance for unmanned surface vehicles," DTIC Document, Tech. Rep., 2007.

[13] C. Goerzen, Z. Kong, and B. Mettler, "A survey of motion planning algorithms from the perspective of autonomous UAV guidance," *Journal of Intelligent & Robotic Systems*, vol. 57, no. 1, pp. 65–100, 2010.

[14] P. Švec, M. Schwartz, A. Thakur, and S. K. Gupta, "Trajectory planning with look-ahead for unmanned sea surface vehicles to handle environmental disturbances." in *IEEE/RSJ International Conference on Intelligent Robots and Systems (IROS'11)*, September 2011.

[15] P. Švec, A. Thakur, B. C. Shah, and S. K. Gupta, "Trajectory planning for time varying motion goal in an environment with obstacles," in *ASME 2012 International Design Engineering Technical Conferences (IDETC '12) & Computers and Information in Engineering Conference (CIE '12)*, August 12-15 2012.

[16] A. Thakur, P. Švec, and S. Gupta, "GPU based generation of state transition models using simulations for unmanned surface vehicle trajectory planning," *Robotics and Autonomous Systems*, vol. 60, no. 12, pp. 1457–1471, 2012.

[17] D. Wilkie, J. Van Den Berg, and D. Manocha, "Generalized velocity obstacles," in *IEEE/RSJ International Conference on Intelligent Robots and Systems (IROS'09)*, 2009, pp. 5573–5578.

[18] M. R. Benjamin, J. J. Leonard, J. A. Curcio, and P. M. Newman, "A method for protocol-based collision avoidance between autonomous marine surface craft," *Journal of Field Robotics*, vol. 23, no. 5, pp. 333–346, 2006.

[19] J. Larson, M. Bruch, and J. Ebken, "Autonomous navigation and obstacle avoidance for unmanned surface vehicles," DTIC Document, Tech. Rep., 2006.

[20] Y. Kuwata, M. T. Wolf, D. Zarzhitsky, and T. L. Huntsberger, "Safe maritime navigation with COLREGs using velocity obstacles," in *IEEE/RSJ International Conference on Intelligent Robots and Systems (IROS'11)*, 2011, pp. 4728–4734.

[21] T. Fossen, *Guidance and control of marine vehicles*, 1st Ed. Wiley, 1994.

[22] J. Alvarez, I. Bertaska, and K. von Ellenrieder, "Nonlinear adaptive control of an amphibious vehicle," in *ASME Dynamic Systems and Control Conference (DSCC'13)*, Stanford University, Palo Alto, CA, October 21-23 2013.

[23] I. Bertaska, J. Alvarez, S. Armando, K. D. von Ellenrieder, M. Dhanak, B. Shah, P. Švec, and S. K. Gupta, "Experimental evaluation of approach behavior for autonomous surface vehicles," in *ASME Dynamic Systems and Control Conference (DSCC'13)*, Stanford University, Palo Alto, CA, October 21-23 2013.

[24] A. S. Huang, E. Olson, and D. C. Moore, "LCM: Lightweight communications and marshalling," in *IEEE/RSJ International Conference on Intelligent Robots and Systems (IROS'10)*, 2010, pp. 4057–4062.